

CERN LHC analysis of the strongly interacting WW system: Gold-plated modes

J. Bagger,¹ V. Barger,² K. Cheung,³ J. Gunion,⁴ T. Han,⁴ G. A. Ladinsky,⁵
R. Rosenfeld⁶ and C.-P. Yuan⁷

¹*Department of Physics and Astronomy, Johns Hopkins University, Baltimore, Maryland 21218*

²*Department of Physics, University of Wisconsin, Madison, Wisconsin 53706*

³*Center for Particle Physics, University of Texas at Austin, Austin, Texas 78712*

⁴*Davis Institute for High Energy Physics, Department of Physics,
University of California at Davis, Davis, California 95616*

⁵*Department of Physics and Astronomy, Michigan State University, East Lansing, Michigan 48824*

⁶*Instituto de Física, Universidade de Sao Paulo, P.O. Box 20516, Sao Paulo, Brazil*

(Received 1 May 1995)

We study the gold-plated purely leptonic signal and background rates at the CERN, LHC for the ZZ , W^+W^- , $W^\pm Z$, and $W^\pm W^\pm$ final states associated with strongly interacting electroweak symmetry breaking. We work at an energy of $\sqrt{s} = 14$ TeV, and develop a combination of back-to-back leptonic, central-jet-vetoing and forward-jet-tagging cuts that suppresses the standard-model backgrounds. We find that the LHC with an annual luminosity of 100 fb^{-1} will achieve a reasonably good sensitivity to the physics of strongly interacting electroweak symmetry breaking.

PACS number(s): 13.85.Qk, 12.60.Fr, 13.38.Dg, 14.80.Bn

I. INTRODUCTION

In a recent paper [1], we studied the signals and backgrounds for strongly interacting electroweak symmetry breaking [2, 3] at hadron supercolliders. We analyzed WW scattering in a series of models that are consistent with present data. (In this paper, the symbol W denotes either W^\pm or Z , unless specified otherwise.) We concentrated on the gold-plated purely leptonic decays of the final-state W 's, e.g., $W^\pm \rightarrow \ell^\pm \nu$ and $Z \rightarrow \ell^+ \ell^-$ ($\ell = e, \mu$) to avoid large QCD backgrounds. We developed a set of techniques, including back-to-back leptonic, forward-jet-tagging and central-jet-vetoing cuts, that proved sufficient to isolate the strongly interacting signal from the standard-model background. For each model, we found a statistically significant sensitivity in at least one channel.

In our previous work, our cuts were optimized for the Superconducting Super Collider (SSC) environment. Nevertheless, we found significant signals at a CERN Large Hadron Collider LHC energy of $\sqrt{s} = 16$ TeV, assuming an annual luminosity of 100 fb^{-1} . In this paper, we refine our LHC analysis using the currently planned energy of $\sqrt{s} = 14$ TeV. As before, we consider seven different models to represent the possible physics associated with a strongly interacting electroweak symmetry breaking sector.

(1) SM: The standard model with $M_H = 1$ TeV.

(2) Scalar: A nonlinearly realized chiral model with a spin-zero, isospin-zero resonance of mass $M_S = 1$ TeV and width $\Gamma_S = 350$ GeV.

(3) $O(2N)$: A large- N model [4] that gives rise to an amplitude with a pole at $s = [M - i\Gamma/2]^2$, where $M = 0.8$ TeV and $\Gamma = 600$ GeV for $N = 2$ and high-energy cutoff $\Lambda = 3$ TeV.

(4) Vector: A nonlinearly realized chiral model with a spin-one, isospin-one resonance; we choose the mass-

width combinations $(M_V, \Gamma_V) = (1 \text{ TeV}, 5.7 \text{ GeV})$ and $(2.5 \text{ TeV}, 520 \text{ GeV})$.

(5) LET-CG: A nonresonant nonlinearly realized chiral model based on the low energy theorems (LET's) for Goldstone boson scattering. The scattering amplitudes are unitarized by cutting off the tree-level partial waves when they reach the unitarity bound [3].

(6) LET- K : The same model as above, except that the scattering amplitudes are unitarized by the K -matrix technique.

(7) Delay- K : A nonresonant nonlinearly realized chiral model in which the scattering amplitudes are computed to second order in the energy expansion. The counterterms are chosen to delay the unitarity violation to energies beyond 2 TeV [5]. K -matrix unitarization is used to ensure unitarity beyond this point.

These models are described fully in Ref. [1].

For each of these models, we consider the final-state modes

$$ZZ \rightarrow \ell^+ \ell^- \ell^+ \ell^-, \quad ZZ \rightarrow \ell^+ \ell^- \nu \bar{\nu}, \quad W^\pm Z \rightarrow \ell^\pm \nu \ell^+ \ell^-, \\ W^+ W^- \rightarrow \ell^+ \nu \ell^- \bar{\nu}, \quad W^\pm W^\pm \rightarrow \ell^\pm \nu \ell^\pm \nu.$$

We include the process $ZZ \rightarrow \ell^+ \ell^- \nu \bar{\nu}$ [6] to enhance the statistical significance of the ZZ channel. For the models with vector resonances, we also compute $q\bar{q}' \rightarrow W^* \rightarrow V \rightarrow WW$ [7, 8]. This $q\bar{q}$ annihilation process is more important at LHC than SSC energies.

Our background analysis includes the "irreducible electroweak (EW)" processes, $q\bar{q}' \rightarrow q\bar{q}' W_T W_T$ ($W_T W_L$), and the "continuum WW " processes, $q\bar{q}' \rightarrow WW + \text{QCD jets}$. We reevaluate the continuum contribution to include all $O(\alpha_s)$ corrections [9], which are important in the kinematical region of interest. We also update the top quark backgrounds, $t\bar{t} + \text{jets}$ and $t\bar{t}W + \text{jets}$, for $m_t = 175$ GeV. Finally, we include a new detector-dependent background, $W^+ Z \rightarrow \ell^+ \ell^+ X$. This is a background to the $W^+ W^+$ final state [10, 8]. In our numerical calculations,

we use the recent parton distribution functions Martin-Roberts-Stirling (MRS) set-A [11]. Other recent work along similar lines can be found in Refs. [8, 10].

II. WW FUSION

At hadron supercolliders, the physics of strongly interacting electroweak symmetry breaking can be studied through the fusion of two longitudinally polarized W 's. These particles interact and then rescatter into the final state. The final-state W 's then decay to leptons, giving events that are characterized by several distinct features which can be used to separate the signal from the background [12, 13].

(i) The signal events contain very energetic leptons in the central (low-rapidity) region. The leptons from W^+W^- and $W^\pm W^\pm$ are very back-to-back, so $\cos\phi_{\ell\ell}$ is near -1 and $\Delta p_T(\ell\ell) \equiv |\mathbf{p}_T(\ell_1) - \mathbf{p}_T(\ell_2)|$ is large ($\phi_{\ell\ell}$ is the azimuthal angle between a lepton ℓ_1 from one W_L and a lepton ℓ_2 from the other). The invariant mass $M(\ell\ell)^2 = (p_{\ell_1} + p_{\ell_2})^2$ is large as well.

(ii) The signal events have low hadronic jet activity in the central region.

(iii) The signal events also contain two highly energetic, low- p_T , high-rapidity ‘‘spectator’’ jets.

In our previous paper, we found that stringent leptonic

cuts, when combined with a veto of events with hard central jets and a tag of energetic spectator jets, were sufficient to dramatically suppress the large backgrounds. In particular, we found the most difficult irreducible electroweak backgrounds to be those from $W_T W_T$ and $W_T W_L$ final states at $O(\alpha^4)$. These backgrounds have spectator jets that are more central and leptons that are less back-to-back than those from the $W_L W_L$ signal. The central-jet veto plus $\cos\phi_{\ell\ell} < -0.8$ and large- $\Delta p_T(\ell\ell)$ cuts proved to be effective against these important backgrounds. After carefully examining the kinematics of the signal and backgrounds, our reoptimized cuts are summarized in Table I. Note that the transverse mass variables are defined as $M_T^2(ZZ) = [\sqrt{M_Z^2 + p_T^2(\ell\ell)} + \sqrt{M_Z^2 + |p_T^{\text{miss}}|^2}]^2 - [\vec{p}_T(\ell\ell) + \vec{p}_T^{\text{miss}}]^2$, and $M_T^2(WZ) = [\sqrt{M^2(\ell\ell) + p_T^2(\ell\ell)} + |p_T^{\text{miss}}|]^2 - [\vec{p}_T(\ell\ell) + \vec{p}_T^{\text{miss}}]^2$.

As before [1], we use the effective- W approximation (EWA) and the equivalence theorem (ET) to compute the cross sections for the $W_L W_L \rightarrow W_L W_L$ signals. We do this by first computing the cross sections ignoring all jet observables, implementing the lepton cuts by decaying the final-state W_L 's according to their appropriate angular distributions. We then approximate the jet-tagging and vetoing cuts by multiplying our cross sections by tagging and/or vetoing efficiencies determined from an exact SM calculation with a 1 TeV Higgs boson (see Table II).

TABLE I. Leptonic, single-jet-tagging, and central-jet-vetoing cuts for generic $W_L W_L$ fusion processes at the LHC energy, by final-state mode.

	Leptonic cuts	Jet cuts
$ZZ(4\ell)$	$ y(\ell) < 2.5$ $p_T(\ell) > 40$ GeV $p_T(Z) > \frac{1}{4}\sqrt{M^2(ZZ) - 4M_Z^2}$ $M(ZZ) > 500$ GeV	$E(j_{\text{tag}}) > 0.8$ TeV $3.0 < y(j_{\text{tag}}) < 5.0$ $p_T(j_{\text{tag}}) > 40$ GeV No veto
$ZZ(\ell\nu\nu)$	$ y(\ell) < 2.5$ $p_T(\ell) > 40$ GeV $p_T^{\text{miss}} > 250$ GeV $M_T(ZZ) > 500$ GeV $p_T(\ell\ell) > M_T(ZZ)/4$	$E(j_{\text{tag}}) > 0.8$ TeV $3.0 < y(j_{\text{tag}}) < 5.0$ $p_T(j_{\text{tag}}) > 40$ GeV $p_T(j_{\text{veto}}) > 60$ GeV $ y(j_{\text{veto}}) < 3.0$
W^+W^-	$ y(\ell) < 2.0$ $p_T(\ell) > 100$ GeV $\Delta p_T(\ell\ell) > 440$ GeV $\cos\phi_{\ell\ell} < -0.8$ $M(\ell\ell) > 250$ GeV	$E(j_{\text{tag}}) > 0.8$ TeV $3.0 < y(j_{\text{tag}}) < 5.0$ $p_T(j_{\text{tag}}) > 40$ GeV $p_T(j_{\text{veto}}) > 30$ GeV $ y(j_{\text{veto}}) < 3.0$
$W^\pm Z$	$ y(\ell) < 2.5$ $p_T(\ell) > 40$ GeV $p_T^{\text{miss}} > 50$ GeV $p_T(Z) > \frac{1}{4}M_T(WZ)$ $M_T(WZ) > 500$ GeV	$E(j_{\text{tag}}) > 0.8$ TeV $3.0 < y(j_{\text{tag}}) < 5.0$ $p_T(j_{\text{tag}}) > 40$ GeV $p_T(j_{\text{veto}}) > 60$ GeV $ y(j_{\text{veto}}) < 3.0$
$W^\pm W^\pm$	$ y(\ell) < 2.0$ $p_T(\ell) > 70$ GeV $\Delta p_T(\ell\ell) > 200$ GeV $\cos\phi_{\ell\ell} < -0.8$ $M(\ell\ell) > 250$ GeV	$3.0 < y(j_{\text{tag}}) < 5.0$ $p_T(j_{\text{tag}}) > 40$ GeV $p_T(j_{\text{veto}}) > 60$ GeV $ y(j_{\text{veto}}) < 3.0$

This procedure is accurate because the kinematics of the jets in the signal events are determined by the initial-state W_L 's and are insensitive to the strong $W_L W_L$ scattering dynamics in the TeV region.

Since the jet-tagging and vetoing efficiencies are so important for our results, we will review our procedure, focusing on the case of the SM with an ordinary Higgs boson. We start with an exact calculation using the full SM matrix elements of $O(\alpha^4)$ for $q\bar{q}' \rightarrow q\bar{q}' WW \rightarrow q\bar{q}' + 4$ leptons. We include all final-state polarizations, and consider two cases: a heavy 1 TeV Higgs boson, and a light 0.1 TeV Higgs particle.

We evaluate the cross section for the SM with a light Higgs boson because it should accurately represent the perturbative irreducible backgrounds from the $qq' \rightarrow qq' W_T W_T (W_T W_L)$ processes. This background is inevitable because of our inability to experimentally determine the polarizations of the final-state W 's on an event-by-event basis. We emphasize that the rate and kinematical distributions of $W_T W_T (W_T W_L)$ events are quite insensitive to the particular model adopted for strongly interacting $W_L W_L$ scattering.

Given these considerations, we define the $W_L W_L$ signal to be the total enhancement over the SM prediction for a light 0.1 TeV Higgs boson. For the case of 1 TeV Higgs

boson, this implies

$$\sigma(W_L W_L \text{ signal}) \equiv \sigma(\text{SM } M_H = 1 \text{ TeV}) - \sigma(\text{SM } M_H = 0.1 \text{ TeV}). \quad (1)$$

The jet-cut efficiencies are determined from this signal definition. We show in Table II the SM results for the cross sections, after imposing the cuts in Table I. We also show the SM backgrounds as well as the resulting jet-tagging and vetoing efficiencies for a 1 TeV Higgs boson signal. We use these efficiencies for all the models of strong electroweak symmetry breaking.

We summarize some important details regarding our background computations below.

(a) We calculate the background processes for continuum WW production including full one-loop QCD corrections at $O(\alpha^2 \alpha_s)$ [9]. This procedure incorporates large QCD corrections in background rates (as large as 70% for the inclusive cross section), and also allows us to reliably determine the leading-jet kinematics in both the central and forward regions.

(b) As noted earlier, we enhance the utility of the ZZ final states by considering the $ZZ \rightarrow 2\ell 2\nu$ channel [6] as well as the cleaner, but lower rate, $ZZ \rightarrow 4\ell$ mode. For the $ZZ \rightarrow 2\ell 2\nu$ channel there is a detector-dependent

TABLE II. Standard-model cross sections (in fb) for electroweak processes $q\bar{q}' \rightarrow q\bar{q}' WW$, for $M_H = 1$ TeV and 0.1 TeV. Also given are the cross sections for continuum WW production at $O(\alpha^2 \alpha_s)$, and other backgrounds, with $\sqrt{s} = 14$ TeV and $m_t = 175$ GeV.

$ZZ(4\ell)$	Leptonic cuts only	+ Veto only / veto eff.	+ Veto + tag / tag eff.
EW($M_H = 1.0$ TeV)	0.12	-	0.045 / 39%
EW($M_H = 0.1$ TeV)	0.019	-	0.004 / 19%
Continuum ZZ	0.42	-	0.003 / 0.6%
$Z_L Z_L$ signal	0.098	-	0.041 / 43%
$ZZ(2\ell 2\nu)$	Leptonic cuts only	+ Veto only / veto eff.	+ Veto + tag / tag eff.
EW($M_H = 1.0$ TeV)	0.69	0.30 / 43%	0.16 / 54%
EW($M_H = 0.1$ TeV)	0.11	0.014 / 13%	0.006 / 38%
Continuum ZZ	2.2	1.7 / 75%	0.012 / 0.7%
$Z_L Z_L$ signal	0.59	0.29 / 49%	0.16 / 55%
$W^+ W^-$	Leptonic cuts only	+ Veto only / veto eff.	+ Veto + tag / tag eff.
EW($M_H = 1.0$ TeV)	1.1	0.33 / 30%	0.20 / 59%
EW($M_H = 0.1$ TeV)	0.32	0.039 / 12%	0.016 / 40%
Continuum $W^+ W^-$	6.8	3.5 / 51%	0.041 / 1.2%
$t\bar{t}$ + jet	59	0.88 / 1.5%	0.067 / 7.7%
$W_L W_L$ signal	0.80	0.29 / 37%	0.18 / 61%
$W^\pm Z$	Leptonic cuts only	+ Veto only / veto eff.	+ Veto + tag / tag eff.
EW($M_H = 1.0$ TeV)	0.32	0.07 / 22%	0.032 / 46%
EW($M_H = 0.1$ TeV)	0.25	0.043 / 17%	0.018 / 42%
Continuum $W^\pm Z$	3.8	2.2 / 56%	0.03 / 1.4%
$Zt\bar{t}$ + jet	0.42	0.008 / 2.0%	0.001 / 16%
$W_L Z_L$ signal	0.073	0.027 / 37%	0.014 / 52%
$W^\pm W^\pm$	Leptonic cuts only	+ Veto only / veto eff.	+ Veto + tag / tag eff.
EW($M_H = 1.0$ TeV)	0.66	0.15 / 23%	0.099 / 66%
EW($M_H = 0.1$ TeV)	0.45	0.057 / 13%	0.034 / 60%
g exchange	0.15	0.009 / 6.0%	0.001 / 7.7%
$Wt\bar{t}$	0.42	0.012 / 3.0%	0.001 / 13%
Continuum $W^\pm Z$	0.15	0.10 / 65%	0.001 / 1.4%
$W_L W_L$ signal	0.22	0.093 / 43%	0.066 / 70%

TABLE III. Event rates per LHC year for $W_L W_L$ fusion signals from the different models, together with backgrounds, assuming $\sqrt{s} = 14$ TeV, an annual luminosity of 100 fb^{-1} , and $m_t = 175$ GeV. Cuts are listed in Table I. Jet-vetoing and tagging efficiencies are listed in Table II. The $W^\pm Z(M_T^{\text{cut}})$ row refers to the $W^\pm Z$ events with $0.8 < M_T(WZ) < 1.1$ TeV, optimized to search for a 1 TeV isovector signal.

	Bkgd.	SM	Scalar	$O(2N)$	Vec 1.0	Vec 2.5	LET-CG	LET-K	Delay-K
$ZZ(4\ell)$	0.7	9	4.6	4.0	1.4	1.3	1.5	1.4	1.1
$ZZ(2\ell 2\nu)$	1.8	29	17	14	4.7	4.4	5.0	4.5	3.6
W^+W^-	12	27	18	13	6.2	5.5	5.8	4.6	3.9
$W^\pm Z$	4.9	1.2	1.5	1.2	4.5	3.3	3.2	3.0	2.9
$W^\pm Z(M_T^{\text{cut}})$	0.82				2.3				
$W^\pm W^\pm$	3.7	5.6	7.0	5.8	12	11	13	13	8.4

background from Z +QCD jets, where $Z \rightarrow 2\ell$ and the jets are missing along the beampipe or are mismeasured by the calorimeter, resulting in significant missing p_T . Recent studies including detector simulations at the LHC [10, 14] show that this background can be suppressed below that from continuum ZZ production by requiring $p_T^{\text{miss}} > 250$ GeV. Thus, we have imposed this cut and neglected the 2ℓ + QCD jets background.

(c) Obviously, $t\bar{t}$ production overwhelms the $W_L^+ W_L^-$ signal in total rate at the LHC energy. Nonetheless, our combination of stringent leptonic cuts, together with the central-jet veto and forward-jet tag, reduces the background to a manageable level.

(d) The 1 TeV Higgs boson contribution to the SM $W^\pm Z$ process (via t -channel exchange) is hardly significant, so we have optimized our cuts in this channel for a vector resonance signal with $M_V \sim 1$ TeV and $\Gamma_V \sim 5.7$ GeV.

(e) Since $q\bar{q}$ annihilation to $W^\pm W^\pm$ is not possible, the leading QCD-related background comes from diagrams in which a gluon is exchanged between two colliding quarks which then radiate the two like-sign W 's. We denote this by “ g exchange” [15, 16, 12]. We find that our cuts effectively remove this background despite the kinematic similarity of its final state to the WW scattering reaction of interest. This type of process also contributes to all the other channels, but is of higher order, $O(\alpha^2 \alpha_s^2)$, than the continuum WW processes that we include, $O(\alpha^2 \alpha_s)$.

(f) Because of the finite coverage of the EM calorimeter, $|y(\ell)| \sim 3$ [10, 14], one must consider the background to $W^\pm W^\pm$ from $W^\pm Z$ when the extra ℓ^\mp from Z decay is not detected [10, 8]. As we see from Table II, this continuum $W^\pm Z$ background is as large as the $W^\pm W^\pm$ signal

after leptonic and central-jet-vetoing cuts. The most efficient means for removing this background is to include a forward-jet-tagging cut.

In fact, the $W^\pm Z$ process may also be a background to W^+W^- if the ℓ^\pm from Z decay is not detected. However, this is far less important than the $t\bar{t}$ background; therefore it is not surprising that it is eliminated by the stringent leptonic and jet-tagging cuts in the W^+W^- channel.

(g) Of course, we have implicitly assumed sufficiently good isolation for identified charged leptons that faked backgrounds from c, b -quark semileptonic decays are not significant, see Ref. [1].

In Table III and Fig. 1 we present our results for $W_L W_L$ fusion signals versus the SM backgrounds for the different models described above.

The isoscalar models [SM, scalar, $O(2N)$] give rise to substantial signals over backgrounds in the $ZZ \rightarrow 4\ell$ and $ZZ \rightarrow 2\ell 2\nu$ channels. Especially encouraging is the signal rate for the $2\ell 2\nu$ mode. The W^+W^- channel also exhibits some sensitivity to these models; the actual sensitivity is probably somewhat greater since the distribution in the mass variable $M(\ell\ell)$ peaks broadly around half the mass of the scalar resonance.

The isovector models (Vec 1.0, Vec 2.5) yield a continuum event excess in the $W^\pm W^\pm$ channel, and, to a lesser extent, in the $W^\pm Z$ channel, where the signal rates are rather low and the background level remains difficult. Nevertheless, as seen in the M_T distribution for the $W^\pm Z$ channel, it might be possible to search for a signal peak if $M_V \sim 1$ TeV. As indicated by the results in the $W^\pm Z(M_T^{\text{cut}})$ row of Table III, if we concentrate on the transverse mass region of $0.8 < M_T(WZ) < 1.1$

TABLE IV. Number of years (if < 10) at LHC required for a 99% confidence level signal.

Channel	Model							
	SM	Scalar	$O(2N)$	Vec 1.0	Vec 2.5	LET-CG	LET-K	Delay-K
$ZZ(4\ell)$	1.0	2.5	3.2					
$ZZ(2\ell 2\nu)$	0.5	0.75	1.0	3.7	4.2	3.5	4.0	5.7
W^+W^-	0.75	1.5	2.5	8.5		9.5		
$W^\pm Z$				7.5				
$W^\pm W^\pm$	4.5	3.0	4.2	1.5	1.5	1.2	1.2	2.2

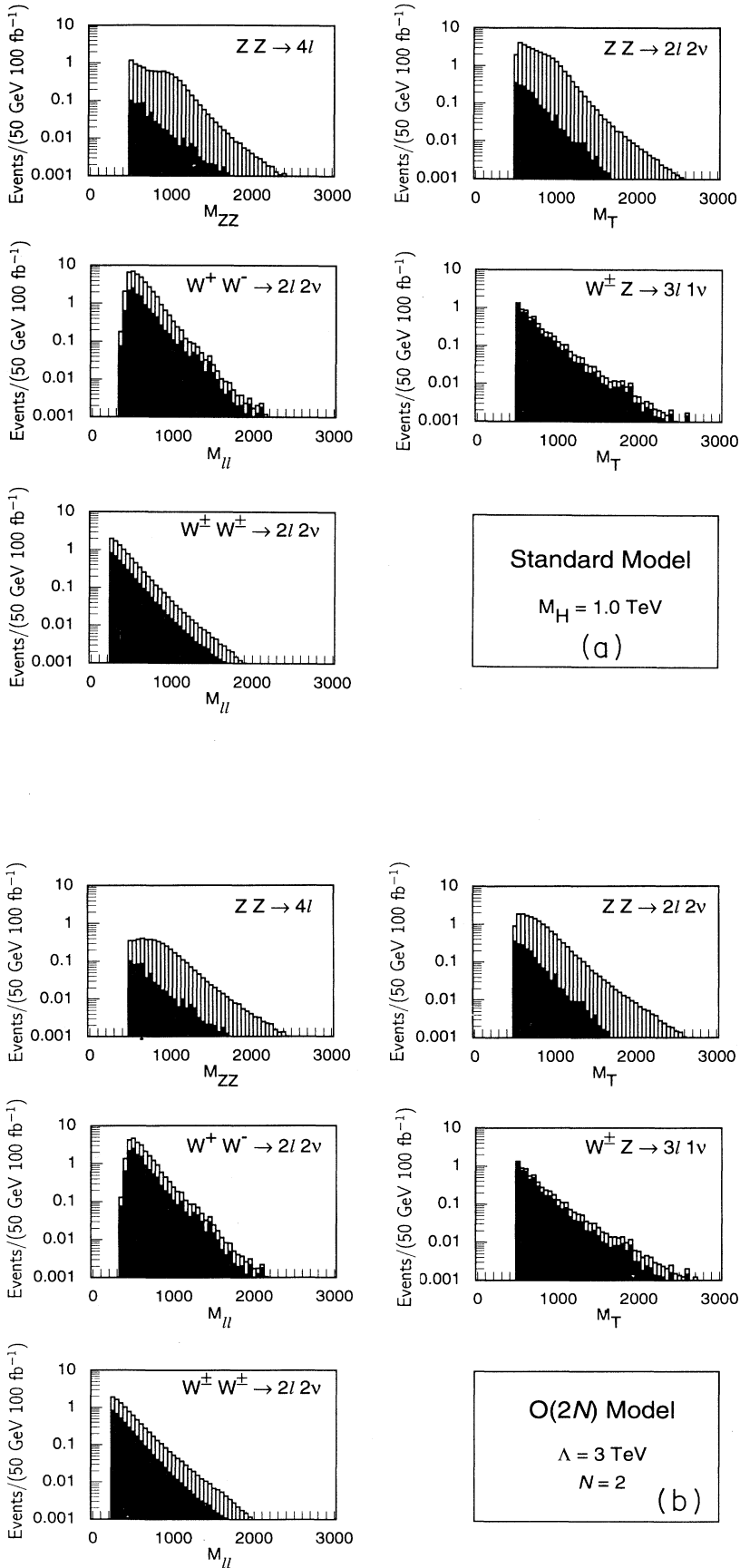


FIG. 1. Invariant mass distributions for the gold-plated purely leptonic final states that arise from the processes $pp \rightarrow ZZX \rightarrow 4\ell X$, $pp \rightarrow ZZX \rightarrow 2\ell 2\nu X$, $pp \rightarrow W^+W^-X$, $pp \rightarrow W^\pm ZX$ and $pp \rightarrow W^\pm W^\pm X$, for $\sqrt{s} = 14 \text{ TeV}$ and an annual LHC luminosity of 100 fb^{-1} . The signal is plotted above the summed background. The mass variable of the x axis is in units of GeV and the bin size is 50 GeV. Distributions are presented for (a) the SM with a 1 TeV Higgs boson; (b) the $O(2N)$ model with $N = 2$ and cutoff $\Lambda = 3 \text{ TeV}$; (c) a chirally coupled scalar with $M_S = 1 \text{ TeV}$, $\Gamma_S = 350 \text{ GeV}$; (d) a chirally coupled vector with $M_V = 1 \text{ TeV}$, $\Gamma_V = 5.7 \text{ GeV}$; (e) a chirally coupled vector with $M_V = 2.5 \text{ TeV}$, $\Gamma_V = 520 \text{ GeV}$; (f) the LET-CG nonresonant model unitarized following Chanowitz and Gaillard; (g) the LET- K nonresonant model unitarized by the K -matrix prescription; (h) the Delay- K $O(p^4)$ nonresonant model, unitarized by the K -matrix prescription.

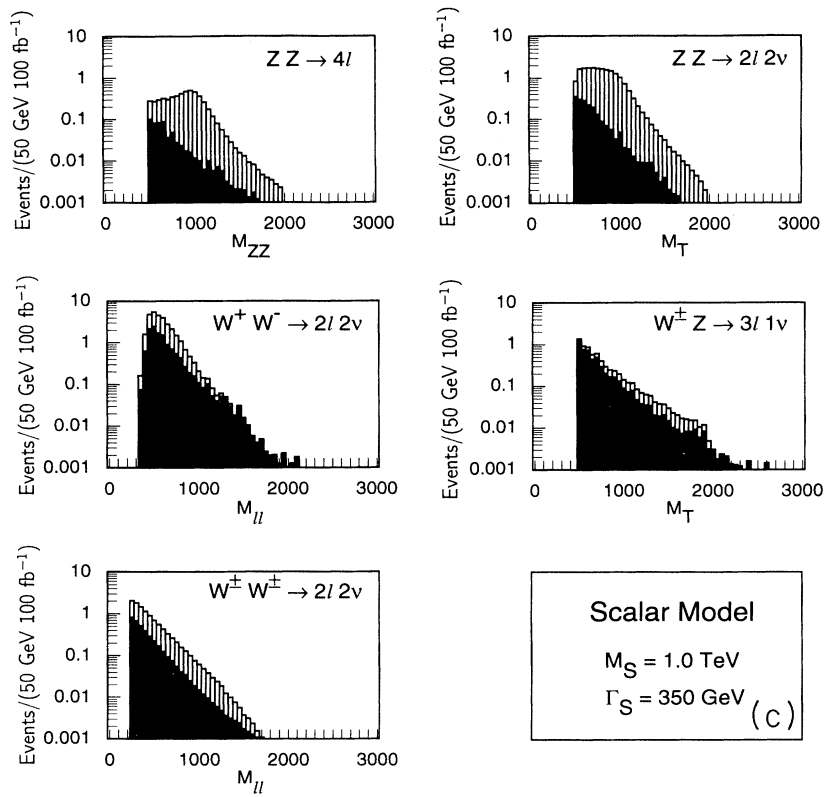
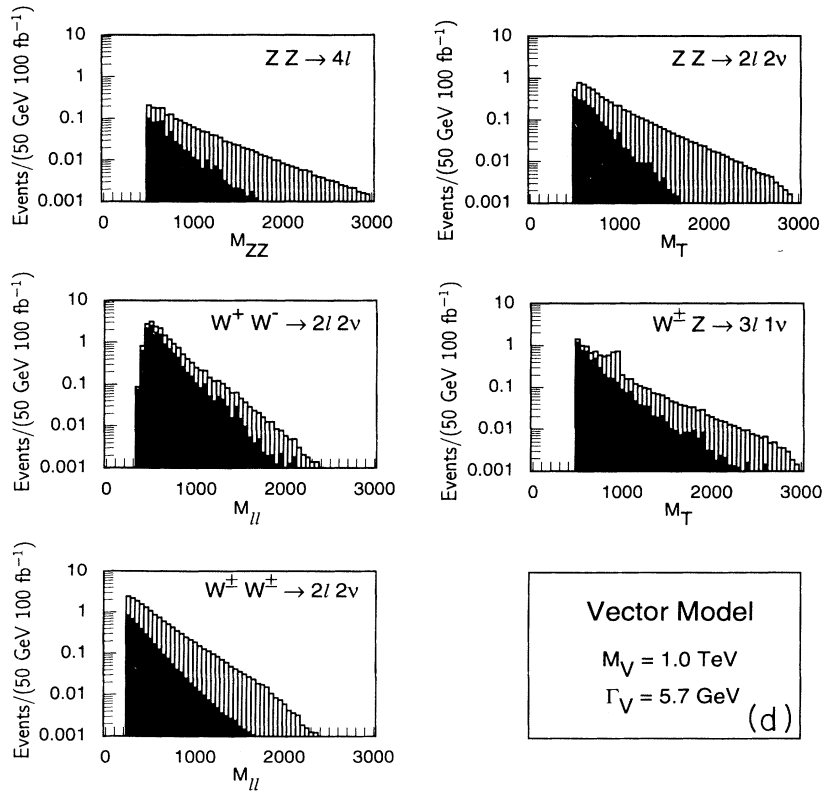


FIG. 1 (Continued).



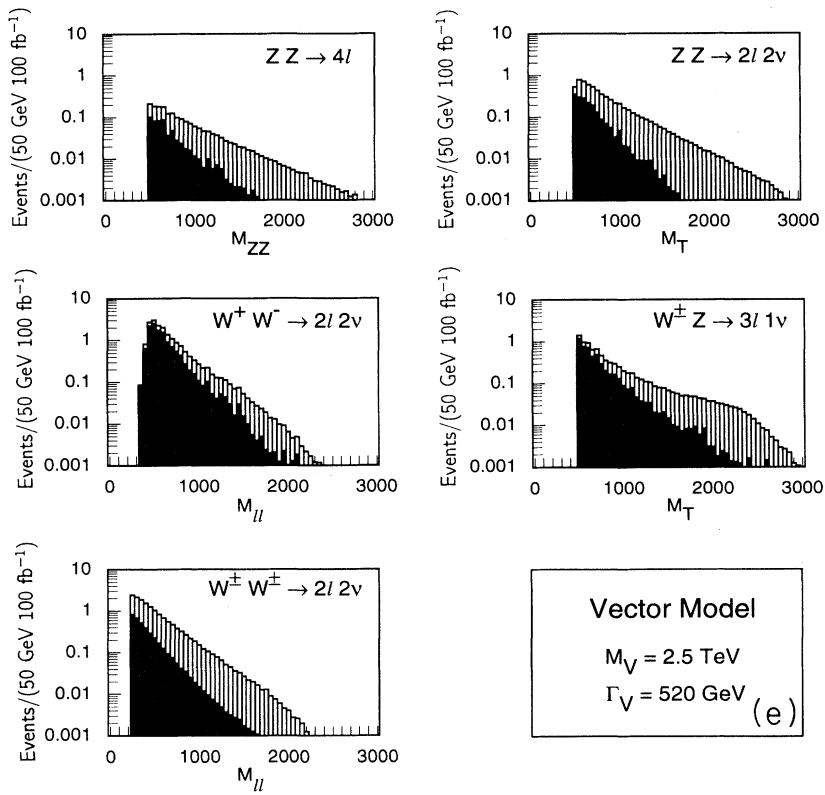
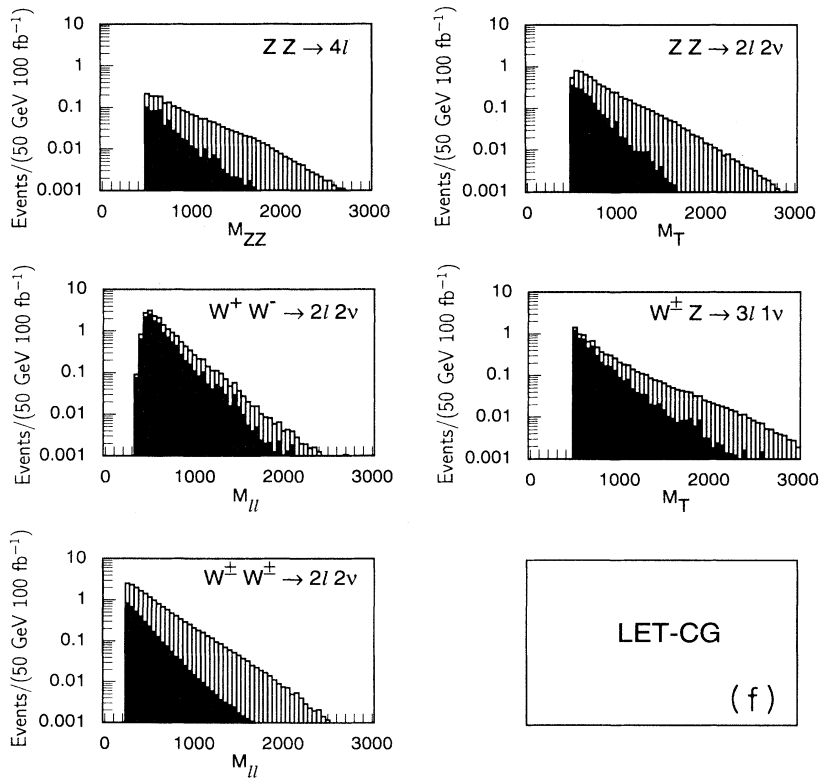


FIG. 1 (Continued).



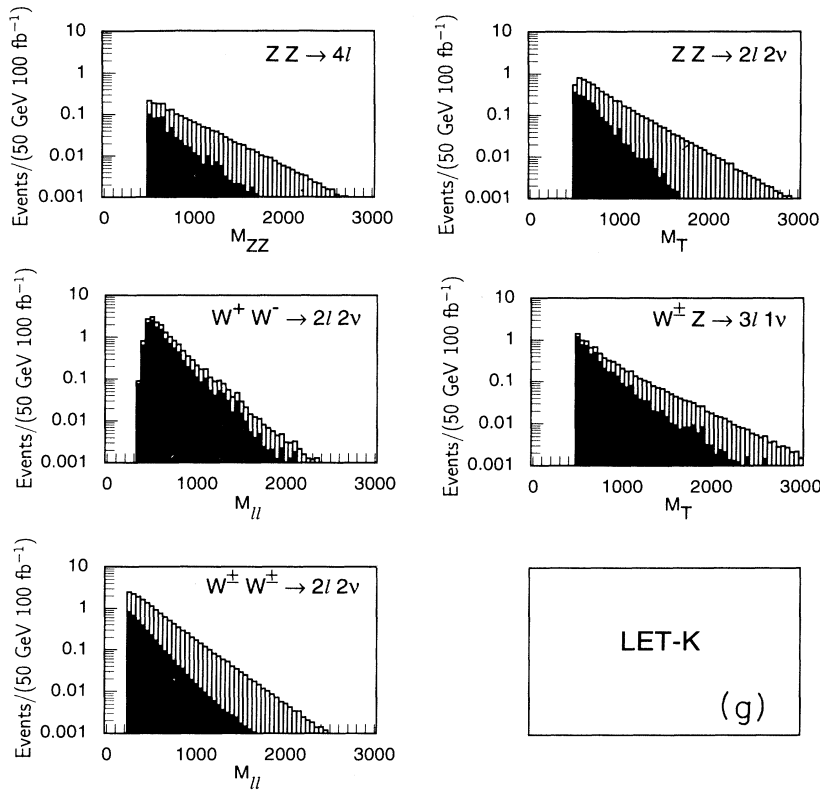
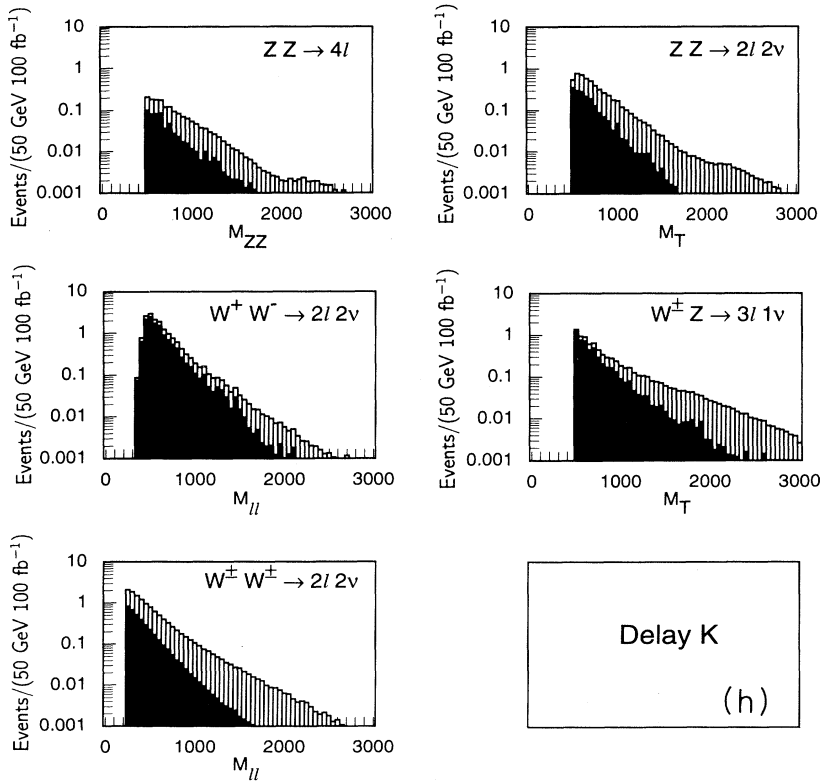


FIG. 1 (Continued).



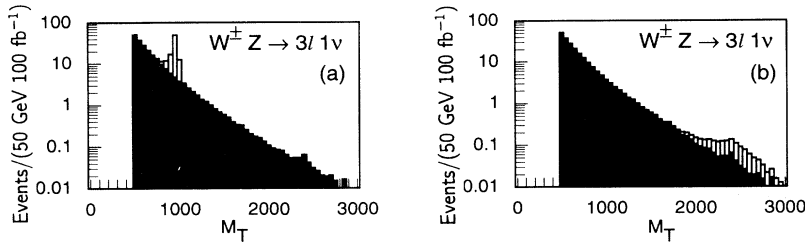


FIG. 2. Transverse mass distributions for $pp \rightarrow W^* - V \rightarrow W^\pm Z X$ signals for (a) $M_V = 1$ TeV, $\Gamma_V = 5.7$ GeV and (b) $M_V = 2.5$ TeV, $\Gamma_V = 520$ GeV. The signal is plotted above the summed SM background. The mass variable of the x axis is in units of GeV and the bin size is 50 GeV.

TeV for a 1 TeV isovector signal, there would be about 0.8 background events and about 2 signal events, for an integrated luminosity of 100 fb^{-1} .

The nonresonant models (LET-CG, LET- K , delay- K) all yield observable excesses in the $W^\pm W^\pm$ channel.

From Table III for the $W_L W_L$ fusion signals and the predicted background rates, we can estimate the number of LHC years necessary to generate a signal at the 99% confidence level defined as follows. We require $B_{\text{max}} < S_{\text{min}}$, where Poisson statistics predicts that 99% of the time pure background would yield $B < B_{\text{max}}$, while signal plus background would yield $S > S_{\text{min}}$. We employ Poisson statistics due to the rather small event rates in certain channels/models. For sufficient S and B event numbers that Gaussian statistics can be employed, our 99% confidence level corresponds roughly to $S/\sqrt{S+B} = 4$, i.e., a statistical significance of 4σ . The results are given in Table IV. We see that with a few years running at the LHC, one should be able to observe a significant enhancement in at least one gold-plated channel. Such an enhancement would be an important step towards revealing the physics of electroweak symmetry breaking.

III. DRELL-YAN PRODUCTION

At the LHC energy, further sensitivity to the isovector models is possible through the Drell-Yan process [7, 8]. Assuming that the vector resonance does not couple directly to the quarks, the Drell-Yan production occurs only through W - V mixing. The spin and color-averaged amplitude for $q\bar{q}' \rightarrow W^* - V \rightarrow W_L^\pm Z_L, W_L^+ W_L^-$ is

$$|\overline{\mathcal{M}}|^2 = \frac{a^2 g^4 (c_v^2 + c_a^2)}{96} \frac{tu}{(s - M_V^2)^2 + M_V^2 \Gamma_V^2},$$

where $c_v = c_a = 1/\sqrt{2}$ for $W^\pm Z$, and $c_v =$

$(1 - \tan^2 \theta_w) t_{3L}^{(i)}$ and $c_a = (1 - \tan^2 \theta_w) [t_{3L}^{(i)} - (2Q_i \sqrt{a} M_Z / M_V) \sin^2 \theta_w]$ for $W^+ W^-$. In the latter case, $Q_i = +\frac{2}{3}$ and $t_{3L}^{(i)} = \frac{1}{2}$ for quark flavors $i = u, c, t$, while $Q_i = -\frac{1}{3}$ and $t_{3L}^{(i)} = -\frac{1}{2}$ for $i = d, s, b$. The constant a is determined by the width and mass of the vector resonance, $a = 192\pi v^2 \Gamma_V / M_V^3$, where $v = 246$ GeV.

If the isovector mass is not too large, the signal from this process may have more statistical significance than that for longitudinal $W^\pm Z$ scattering via WW fusion discussed above. However, we must eliminate the jet tag because the mixing mechanism does not have an accompanying spectator jet at lowest order.

In what follows we present our result from a Born-level calculation for the signal processes, assuming a 100% efficiency for the central-jet veto. This is a reasonable approximation because for $q\bar{q}' \rightarrow WW$ processes, the Born-level result is very close to that of the QCD corrected zero-jet process after vetoing [9, 17]. (Note that the mixing processes do not contribute significantly to our single-tag event rates in Table III. This is because the tagging efficiencies for the mixing processes would be 1.4% and 1.2% in the two channels, respectively, as computed for the continuum WW cross sections.)

In Fig. 2 we show the transverse mass distributions for the sum of the signals and SM backgrounds for $M_V = 1$ TeV and 2.5 TeV. Despite the increase in background that results from eliminating the jet tag, the increase in the signal for a 1 TeV vector resonance presents a clear bump in the M_T spectrum near the resonance mass. As expected, the $W^\pm Z$ channel via W - V mixing could be best for studying a vector resonance at the LHC if its mass is near 1 TeV.

Indeed, from Table V we see that in the bin $0.85 < M_T(WZ) < 1.05$ TeV, the mixing signal has a statistical significance of $S/\sqrt{B} \sim 15$, far better than obtained in any of the channels after single-tagging the spectator jets;

TABLE V. Event rates per LHC year for $q\bar{q} \rightarrow W^+ W^-$ and $q\bar{q}' \rightarrow W^\pm Z$ channels, from W - V mixing and backgrounds, compared to the corresponding $W_L W_L$ fusion signal rates, after removing the jet-tagging cut in Table I, assuming $\sqrt{s} = 14$ TeV, an annual luminosity of 100 fb^{-1} , and $m_t = 175$ GeV.

	Bkgd.	Vec 1.0: W - V mix / fusion	Vec 2.5: W - V mix / fusion
$W^+ W^-$	420	8.6 / 10	0.3 / 9.0
$W^\pm Z$	220	73 / 8.7	1.4 / 6.4
$W^\pm Z$		$0.85 < M_T(WZ) < 1.05$ TeV	$2 < M_T(WZ) < 2.8$ TeV
Bkgd./mix/fusion		22/ 69 / 3.2	0.82/0.81/0.55

see Table III. However, for a 2.5 TeV vector state the signal rate is too low to be observable.

The W^+W^- channel seems to be less useful for observing a vector resonance signal arising via the mixing process. This is a consequence of the more stringent leptonic cuts that are necessary to suppress the larger SM backgrounds (especially the $t\bar{t}$ background), as well as the lack of distinctive peak structure in the $M(\ell\ell)$ distribution. The event rates for signals and backgrounds are shown in Table V.

IV. DISCUSSION

Having presented our results, we will close with a few comments.

(a) A systematic comparison of the different gold-plated modes allows one to distinguish between the different models to a certain degree. Models with a scalar isospin-zero resonance [SM, Scalar and $O(2N)$] will yield a large excess of events in the $ZZ \rightarrow 2\ell 2\nu$, $ZZ \rightarrow 4\ell$, and $W^+W^- \rightarrow \ell^+\ell^-\nu\nu$ final states, a feature that is very distinct from predictions of the other models; those with a vector isospin-one resonance with $M_V \sim 1$ TeV can be studied most easily in the $W^\pm Z \rightarrow \ell^\pm\nu 2\ell$ channel via W - V mixing; while models with heavier vector resonances or no resonances at all imply a large enhancement in the $W^\pm W^\pm \rightarrow \ell^\pm\ell^\pm 2\nu$ channels.

(b) As mentioned previously, we have used EWA and ET techniques to calculate the signal cross sections for all the models. We have checked that for a 1 TeV Higgs boson, and using our cuts, the EWA and ET results agree with the exact SM calculation to about 10% for the non-resonant channels ($W^\pm Z, W^\pm W^\pm$) and to about a factor of 2 for those with an s -channel resonance (ZZ, W^+W^-). The discrepancy is caused by difficulties in treating the large resonant width in the ET formalism. It should be emphasized, however, that the EWA and ET techniques give accurate results for nonresonant channels only in the large M_{WW} and central rapidity regions. On the other hand, we have carried out exact calculations for the $W_T W_T$ and $W_T W_L$ background processes at $O(\alpha^4)$; for these processes EWA calculations are not applicable [15].

(c) For our signal calculations of $W_L W_L$ scattering, we have chosen the QCD scale in the parton distribution functions to be M_W and have ignored higher order QCD effects. It is shown [18] that with such a scale choice, the QCD corrections to the $W_L W_L$ scattering processes are negligible and our signal results are thus of rather small theoretical uncertainty. Moreover, since we have concentrated on the exclusive channels with a tagged jet and (most of the time) vetoing central jets, effects on our analyses from additional QCD radiation are small, for both signal and background processes.

(d) We have found that tagging a single energetic forward jet is effective in suppressing the large backgrounds, especially those from continuum WW production, including $W^\pm Z$ as a background to $W^\pm W^\pm$. Based on results from detector simulations at high luminosities [19, 10, 14], we have taken the jet-tagging threshold to be $p_T(j) > 40$ GeV. Whether it is more advantageous to tag

both of the forward jets, or just one, depends crucially on the minimum $p_T(j)$ threshold below which tagging is not feasible. The $W_L W_L$ scattering signal tends to give jets with quite small p_T ($\langle p_T \rangle \sim M_W/2$), so that many of the spectator jets have p_T 's below 40 GeV. This means that if the minimum p_T threshold is set high ($\gtrsim 40$ GeV), then only single-tagging gives a reasonable efficiency for retaining the signal events of interest. On the other hand, if a much lower p_T threshold can be used, then double-tagging is quite efficient for isolating the $W_L W_L$ signal. In Ref. [10] it is claimed that the pileup background is quite small after *double*-tagging, even for a threshold as low as 15 GeV. If such a low threshold for double-tagging can be employed, one can consider relaxing some of the leptonic cuts to obtain larger signal rates. Note however, that the threshold of 40 GeV we applied refers to a value at the parton level; in contrast, the threshold of 15 GeV of Ref. [10] is imposed after full fragmentation and jet reconstruction, and may correspond to a higher parton-level value. Fragmentation will, of course, spread out the momenta of the spectator jets. We have not attempted to model the effects of fragmentation. However, our parton-level threshold is sufficiently high that it should be easy to implement an appropriate corresponding (presumably lower) threshold for reconstructed spectator jets after fragmentation. This corresponding threshold should be determined using detailed detector Monte Carlo simulations (that also incorporate calorimeter losses and the like) by the ATLAS and CMS detector groups.

Further study will be needed to determine whether isolation of the $W_L W_L$ signal is better accomplished via single-tagging with strong lepton cuts [1] or double-tagging with weaker lepton cuts [10]. In practice, it will undoubtedly prove fruitful to analyze the data following both procedures. However, we wish to emphasize that single-tagging with strong leptonic cuts has the advantage of minimizing the influence of uncertainties associated with $W_T W_T, W_T W_L$ final states. This is because double-tagging with weak leptonic cuts, although yielding a larger signal event rate, has a much smaller ratio of the $W_L W_L$ to the $W_T W_T + W_T W_L$ background. Thus, a 20% change or uncertainty in the transversely polarized W background would be confused with the $W_L W_L$ signal in the case of double-tagging with weak lepton cuts, but not in the single-tagging-strong-lepton-cuts analysis. Uncertainties in the background rate predictions will inevitably be present. In particular, systematic errors in the Monte Carlo simulation predictions for the background levels in the various channels will arise due to uncertainties in parton distribution functions, detector response, higher-order corrections and so forth. In addition, by analyzing the data with strong cuts we are able to separate the effects of new physics contributions to the $W_L W_L$ sector from those that might or might not be present in the $W_T W_T, W_T W_L$ sectors.

(e) For the isovector models considered, we have altered our parameter choices from those considered in Ref. [1]. The larger separation in mass (as compared to our earlier choices of 2.0 and 2.5 TeV) provides a better comparison between resonances with high and moderate

masses. Also, the new widths are significantly smaller than those in our previous work. The new widths are roughly the largest allowed that are consistent with the current experimental limits on mixing [20] between the Z and the neutral vector boson V^0 for the models considered. It is important to note that since cross sections for processes with s -channel vector resonances are roughly proportional to the width, our signal rates are rather small. Were the width constraints relaxed, as possible in other models, the signal rates could be substantially enhanced [8].

(f) For the nonresonant models, we have mainly concentrated on the leading-order universal term in a chiral Lagrangian [21], namely, the LET amplitude. Beyond the leading order, we have considered one special case in which the scattering amplitudes are computed to second order in the energy expansion and the counterterms are chosen to delay the unitarity violation to energies beyond 2 TeV [5]. The motivation is to provide a conservative scenario for the nonresonant model. More generally, one should include any higher-order effects and other nonlinear operators that are present in the chiral Lagrangian; the specific forms for such terms reflect the underlying dynamics of a strongly interacting electroweak symmetry breaking sector [22].

Comparing to the results of Ref. [1], we see that lowering the LHC energy to $\sqrt{s} = 14$ TeV weakens the purely leptonic gold-plated signals for a strongly interacting electroweak symmetry breaking sector. Nonetheless, by careful optimization of the cuts, we find that an observable excess of events can be seen for all of the strongly

interacting models that we consider, after several years of running with an annual luminosity of 100 fb^{-1} . Increased rates and significance would be possible if a much lower threshold for jet tagging were possible, despite the large number of pileup events accompanying the $W_L W_L$ scattering reactions and their backgrounds. We emphasize that the search for strong electroweak symmetry breaking requires, in large part, detecting the signal as only an overall enhancement in rates above the SM backgrounds. Therefore the systematics of the experimental measurements must be fully under control.

ACKNOWLEDGMENTS

We would like to thank J. Ohnemus for providing us with the FORTRAN codes to evaluate the processes $q\bar{q}' \rightarrow WW$ with one-loop QCD corrections, and G. Azuelos for discussions regarding Ref. [10]. The work of J. Bagger was supported in part by NSF Grant No. PHY-9404057. The work of V. Barger was supported in part by DOE Grant No. DE-FG02-95ER40896. The work of K. Cheung was supported in part by DOE-FG03-93ER40757. The work of J. Gunion and T. Han was supported in part by DOE Grant No. DE-FG-03-91ER40674. The work of G. Ladinsky was supported in part by NSF Grant No. PYH-9209276. The work of R. Rosenfeld was supported by CNPq in Brazil. C.-P. Yuan was supported in part by NSF Grant No. PHY-9309902. Further support was provided to J. Gunion and T. Han by the Davis Institute for High Energy Physics and to V. Barger by the Wisconsin Alumni Research Foundation.

-
- [1] J. Bagger, V. Barger, K. Cheung, J. Gunion, T. Han, G. Ladinsky, R. Rosenfeld, and C.-P. Yuan, *Phys. Rev. D* **49**, 1246 (1994).
 - [2] D. A. Dicus and V. S. Mathur, *Phys. Rev. D* **7**, 3111 (1973); B. W. Lee, C. Quigg, and H. Thacker, *ibid.* **16**, 1519 (1977); M. Veltman, *Acta Phys. Pol. B* **8**, 475 (1977).
 - [3] M. S. Chanowitz and M. K. Gaillard, *Nucl. Phys.* **B261**, 379 (1985).
 - [4] M. Einhorn, *Nucl. Phys.* **B246**, 75 (1984); S. Naculich and C.-P. Yuan, *Phys. Lett. B* **293**, 395 (1992).
 - [5] J. Bagger, S. Dawson, and G. Valencia, in *Research Directions for the Decade*, Proceedings of the Summer Study, Snowmass, Colorado, 1990, edited by E. Berger (World Scientific, Singapore, 1992).
 - [6] R. N. Cahn and M. Chanowitz, *Phys. Rev. Lett.* **56**, 1327 (1986); V. Barger, T. Han, and R. Phillips, *Phys. Rev. D* **36**, 295 (1987); M. Berger and M. Chanowitz, *Phys. Rev. Lett.* **68**, 757 (1992).
 - [7] R. S. Chivukula, in *The Storrs Meeting*, Proceedings of the Meeting of the Division of Particles and Fields of the APS, Storrs, Connecticut, 1988, edited by K. Haller *et al.* (World Scientific, Singapore, 1989), p. 723; K. Lane and E. Eichten, *Phys. Lett. B* **222**, 274 (1989); R. Casalbuoni *et al.*, *ibid.* **249**, 130 (1990); **253**, 275 (1991); J. Bagger, T. Han, and R. Rosenfeld, in *Research Directions for the Decade* [5]; A. Dobado, M. Herrero, and J. Terron, *Z. Phys. C* **50**, 465 (1991).
 - [8] M. Chanowitz and W. Kilgore, *Phys. Lett. B* **322**, 147 (1994); LBL Report No. LBL-36334 (unpublished).
 - [9] J. Ohnemus, *Phys. Rev. D* **50**, 1931 (1994).
 - [10] ATLAS Collaboration, Technical Proposal, CERN Report No. CERN/LHCC/94-13 (unpublished); ATLAS Internal Note PHYS-NO-033 (unpublished).
 - [11] A. D. Martin, R. G. Roberts, and W. J. Stirling, *Phys. Rev. D* **50**, 6734 (1994).
 - [12] V. Barger, K. Cheung, T. Han, and R. J. N. Phillips, *Phys. Rev. D* **42**, 3052 (1990); D. Dicus, J. F. Gunion, and R. Vega, *Phys. Lett. B* **258**, 475 (1991); D. Dicus, J. F. Gunion, L. H. Orr, and R. Vega, *Nucl. Phys.* **B377**, 31 (1991); M. S. Berger and M. S. Chanowitz, *Phys. Lett. B* **263**, 509 (1991).
 - [13] V. Barger, K. Cheung, T. Han, J. Ohnemus, and D. Zeppenfeld, *Phys. Rev. D* **44**, 1426 (1991); V. Barger, K. Cheung, T. Han, and D. Zeppenfeld, *ibid.* **44**, 2701 (1991); **48**, 5433 (1993).
 - [14] CMS Collaboration, Technical Proposal, CERN Report No. CERN/LHCC/94-38 (unpublished).
 - [15] J. F. Gunion, J. Kalinowski, and A. Tofghi-Niaki, *Phys. Rev. Lett.* **57**, 2351 (1986).
 - [16] D. A. Dicus and R. Vega, *Phys. Lett. B* **217**, 194 (1989).
 - [17] U. Baur, T. Han, and J. Ohnemus, *Phys. Rev. D* **51**,

- 3381 (1995).
- [18] T. Han, G. Valencia, and S. Willenbrock, *Phys. Rev. Lett.* **69**, 3274 (1992).
- [19] SDC Collaboration, Technical Design Report, SDC Report No. SDC-92-201 (unpublished).
- [20] R. Casalbuoni *et al.*, *Phys. Lett. B* **269**, 361 (1991); D. Dominici, in *The Albuquerque Meeting*, Proceedings of the Meeting of the Division of Particles and Fields of the APS, Albuquerque, New Mexico, 1994, edited by S. Seidel (World Scientific, Singapore, 1995).
- [21] T. Appelquist and C. Bernard, *Phys. Rev. D* **22**, 200 (1980); A. Longhitano, *Nucl. Phys.* **B188**, 118 (1981); A. Dobado and M. Herrero, *Phys. Lett. B* **228**, 495 (1989); A. Dobado, M. Herrero, and J. Terron, *Z. Phys. C* **50**, 205 (1991); S. Dawson and G. Valencia, *Nucl. Phys.* **B348**, 23 (1991); **B352**, 27 (1991); J. Bagger, S. Dawson, and G. Valencia, *ibid.* **B399**, 346 (1993); T. Appelquist and G.-H. Wu, *Phys. Rev. D* **48**, 3235 (1993).
- [22] H.-J. He, Y.-P. Kuang, and C.-P. Yuan, Report No. VPI-IHEP-95-05, 1994 (unpublished).